

Effect of Rare-earth Salts on Corrosion Resistance of Phytic Acid Based Conversion Coatings on Q235 Steel

Yong Lu^{1,2}, Huixia Feng^{1,*}

¹ School of Petrochemical Engineering, Lanzhou University of Technology, Gansu China

² Research Institute of Lanzhou Petrochemical Corporation of Petrochina, Gansu China

*E-mail: fenghx66@163.com

Received: 18 March 2020/ Accepted: 8 May 2020 / Published: 10 July 2020

Synergistic effect of rare earth salts conversion coating with phytic acid conversion coating was studied. Rare-earth salts were used as post-treatment to modify the phytic acid coated steel. The corrosion resistance properties of different coatings was investigated with electrochemical impedance spectroscopy in 3.5 wt.% NaCl solution. The corrosion resistance of phytic acid coated steel on steel was further enhanced with cerium nitrate post-treatment. The corrosion rate of phytic acid coated steel was seriously impaired by cerium nitrate post-treatment. But scanning electron microscopy (SEM) images indicated that there are also some micro-cracks on the coating surface when phytic acid coated steel was post-treated with cerium nitrate conversion bath. X-ray photoelectron spectroscopy (XPS) results demonstrated that the phytic acid could bind to the steel surface through the formation of -P-O-Fe and the cerium salts on the steel surface existed in the forms of both Ce³⁺ and Ce⁴⁺.

Keywords: conversion coating, phytic acid, rare-earth salts, corrosion

1. INTRODUCTION

Conversion coating technology is an effective method which has been used in anti-corrosion treatment on metal surface, wear resistance, anti-friction and the bottom coating. Conversion coating not only can temporarily protect substrate from corrosion in corrosive medium, but also can further improve adhesion ability between metal substrate and the subsequent coating layer. That can be used as bottom of subsequent coating processing[1]. Involve in automobile manufacturing, household appliances, hardware processing and many other industries.

Chromate and phosphate was the most widely used kinds of chemical conversion film-forming materials. There is highly toxic hexavalent chromium in the chromate treatment solution, which can lead to genetic defects, even can cause cancer, have lasting harm to the environment and gradually be banned. For phosphate coating, due to the discharge of inorganic phosphate which can pollute the

water bodies seriously[2]. The development and application of green environment-friendly metal surface pretreatment technology has become a very important research orientation in the field of metal surface treatment.

Phytic acid is a non-toxic natural organic macromolecule which can dissolve in water and widely exists in legumes, such as corn, soybeans and nuts[3]. As a kind of metal chelator [4], a phytic acid molecule contains six phosphate groups. Each of the phosphate group have two hydroxies and four oxygen atoms than can chelate with most of the bivalent or trivalent metal ions to form stable complexes in a wide range of pH value. Including Cu^{2+} [5], Zn^{2+} [6], Fe^{2+} , Fe^{3+} [7-9], Al^{3+} [10], Ca^{2+} [11], Mg^{2+} . Phytic acid can be used to treat steel, aluminum alloy, magnesium alloy, copper and other metals. Phytic acid contains abundant hydroxyl groups and phosphate groups that can effectively chemical cross-linking with the subsequent organic coating and the adhesion between the metal surface can be obviously enhanced. Nonetheless, there are some shortcomings in the application of anti-corrosion. There are some micro-cracks under certain conditions that make its protection efficiency is limited and further promotion and application are confined in the field of metal surface pretreatment[12, 13].

So as to improve the protection efficiency of the conversion coating, phytic acid synergistic with other film-forming materials has been applied to anti-corrosion protection of the metal. Gao.[14] deposited a cerium conversion coating and the phytic acid composite conversion sample on an AZ31B magnesium alloy and studied the corrosion resistance of the composite coating in the electrolyte solution. Liu.[15] treated phytic acid conversion coatings on magnesium surface with cerium chloride solution. Mohammadloo.[16] constructed nano-structured titanium-phytic acid conversion coating for cold rolled steel. Corrosion behavior of composite conversion coating has significant improvement than the only phytic acid based coating. Meanwhile, rare-earth salts are expected to be less environmentally harmful that can retard the corrosion rate of several metals. The rare earth conversion coatings, especially in the case of lanthanum[17], praseodymium[18], neodymium [19], samarium[20] and yttrium[21], have been applied to anti-corrosion research on different metal surfaces. But to the best of our knowledge, there has been relatively little scientific study of the effect of rare-earth salts on the tightness and corrosion behavior of phytic acid coated Q235 steels sample. In the present work, synergistic effect of phytic acid conversion coating and rare earth conversion coating is reported. Rare earth salts solution was applied to further enhance the corrosion resistance of phytic acid conversion coating and reduce the micro-cracks of the phytic acid coated Q235 steel. The corrosion behavior of the bare steel and the samples coated with phytic acid(PA)or phytic acid-cerium (composite coating) was investigated through electrochemical impedance spectroscopy(EIS) and potentiodynamic polarization test in 3.5 wt.% NaCl solution. The micro-morphology, elemental chemical states and element composition of the composite coating were observed by the surface analysis technologies of scanning electron microscopy(SEM), X-ray photoelectron spectroscopy(XPS) and X-ray energy dispersive spectrum(EDS), respectively[22].

2.3 Methods of Characterization

The micro-morphology and the chemical composition of the coatings were evaluated via SEM (Hitachi JSM-5600LV, JEOL, Japan) coupled with energy dispersive X-ray spectrum (EDS). The chemical composition of the coating was analyzed using X-ray photoelectron spectroscopy (XPS, Thermo, ESCALAB 250Xi, USA) with a monochromated Al K α ($h\nu=1486.6\text{eV}$) beam and all spectra were corrected using the signal of C1s at 284.8 eV. The curve fitting of the XPS spectra was performed by XPSPEAK 4.1 software.

2.4 Electrochemical corrosion test

A conventional three-electrode cell assembly was used for all electrochemical experiments. The tests were performed on three specimens to ensure the reliability of results. Steel electrode was immersed in the 3.5% NaCl at 25°C as a working electrode. A platinum sheet was used as an auxiliary electrode and a saturated calomel electrode (SCE) as a reference electrode, respectively. Electrochemical impedance spectroscopy(EIS) and potentiodynamic polarization measurements were carried out using a computer-controlled CHI660E electrochemical workstation at room temperature. Prior to each sample for EIS test, the working electrode was immersed in the electrolyte solution for 30 min to attain the steady-state potential. EIS studies were carried out at amplitude and frequency range of ± 5 mV and 10 kHz - 0.01 Hz, respectively. The software ZSimpWin was used to evaluate the obtained parameters by fitting the experimental data. Values of charge transfer resistance (R_{ct}) were obtained from the Nyquist plots by determining the difference in the values of impedance at low and high frequencies. Then the corrosion protection efficiency (E.%) was determined from the R_{ct} using following equation. Polarization testing was implemented at a scanning rate of 0.5 mV/s from -300 mV up to +300 mV around open circuit potential and corrosion current density (I_{corr}) was obtained by extrapolation of Tafel lines.

$$(E.\%) = \frac{R_{ct} - R'_{ct}}{R_{ct}} \times 100\% \quad [1]$$

Where R_{ct} and R'_{ct} denotes the charge transfer resistance values of different coatings, respectively.

The protection efficiency(E.%) was also calculated using the following equation equation:

$$E.(\%) = \frac{I_{\text{bare steel}} - I_{\text{coating}}}{I_{\text{bare steel}}} \times 100\% \quad [2]$$

Where $I_{\text{bare steel}}$ and I_{coating} are the corrosion current densities of bare steel and coated steel, respectively.

3.RESULTS AND DISCUSSION

3.1 Corrosion performance

3.1.1 Electrochemical impedance spectroscopy measurements of different conversion coatings

Cerium nitrate was used for additive, pre-treatment and post-treatment to optimize the process to obtain a more corrosion resistance conversion coating. Other conditions are the same as the conditions of phytic acid treatment. The electrochemical impedance spectra of different coatings are shown in Fig.2.

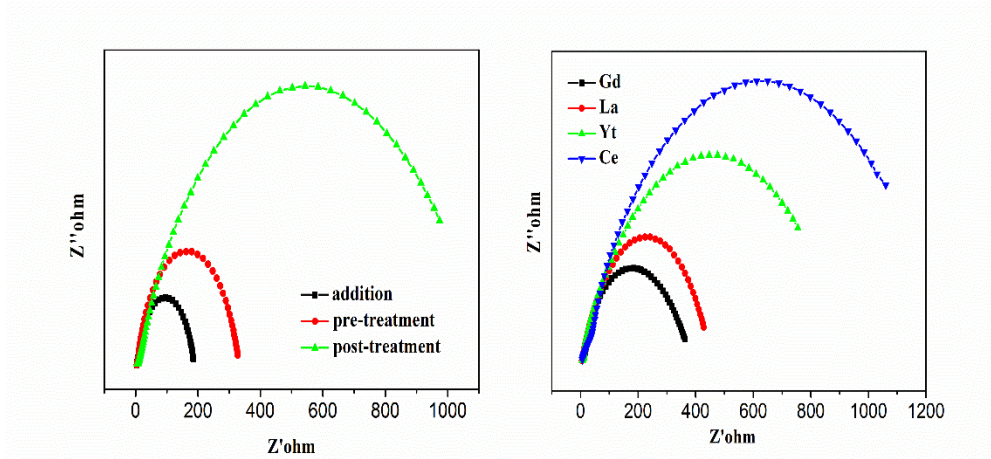


Figure 2. Impedance diagrams of conversion coating (a) prepared by three different processes; (b) Utilization of four different rare-earth salts as a conversion post-treatment

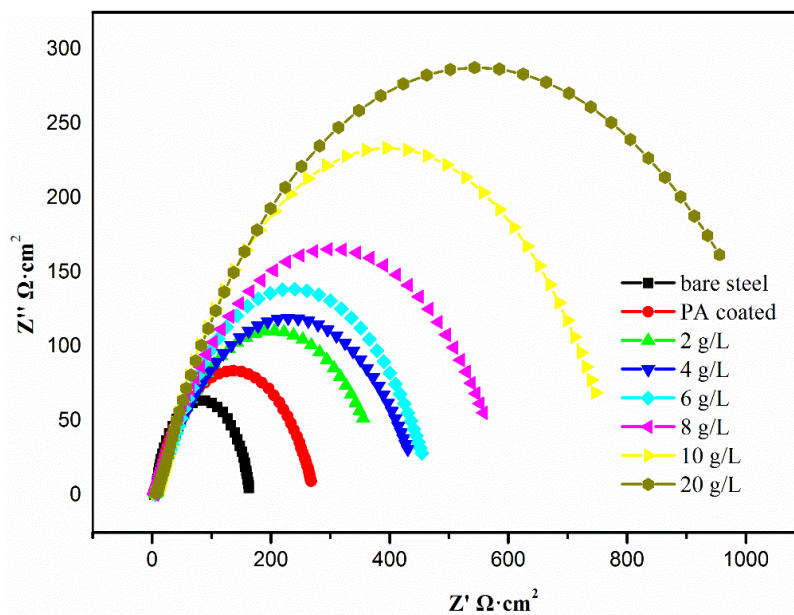


Figure 3. Impedance diagrams of conversion coating of post-treated with different cerium nitrate concentration

It is obvious from the impedance diagrams that the charge transfer resistance value of the conversion coating is quite different after different processes and different rare earth salt treatments. Indicate that phytic acid coated sample was post-treatment with cerium nitrate has better corrosion

resistance against corrosive ion. Therefore, when phytic acid coated steel was post-treated with cerium nitrate solution, the corrosion resistance of the prepared composite conversion coating is much better than other composite coatings. And then compared the corrosion behavior of the coated steel substrates that post-treated with different concentrations of cerium nitrate conversion bath (from 2 g/L to 20 g/L). Nyquist spectrums for coated steel in 3.5.% NaCl of different coatings are shown in Fig.3.

It is clear from the Nyquist plots presented in Fig. 3 that the corrosion resistance of the phytic acid coated steel was post-treated with different cerium nitrate concentration is enhanced to a certain extent. When the concentration of cerium nitrate treatment solution is continuously increased, the corrosion resistance of the obtained composite coating is gradually improved. According to the characteristics of the impedance spectra, the equivalent circuit for studies is shown in Fig.4.

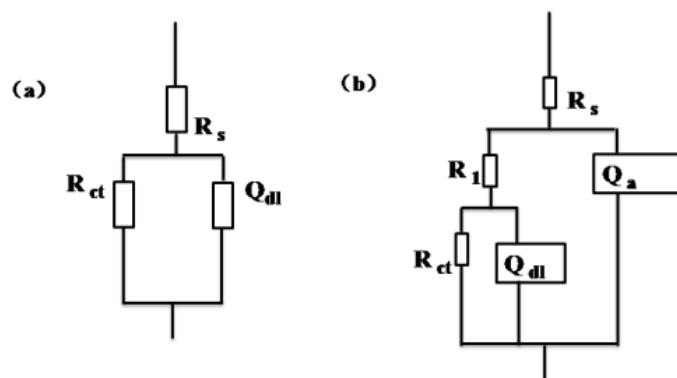


Figure 4. The equivalent circuit models for data fitting

In this equivalent circuit, R_s is the resistance of the electrolyte resulting from the ohmic or uncompensated resistance of the solution between the working and reference electrodes. R_1 and Q_a are the resistance and capacitance of the micro-pores in the coating formed on the steel surface, respectively. Q_{dl} is a constant phase element (CPE) that was included in the fitting instead of an ideal capacitor to simulate the double-layer capacitance at the steel/solution interface. R_{ct} represents the charge transfer resistance at the interface between steel substrate and electrolyte at the crack location of the coating, which is in parallel with the double-layer capacitance Q_{dl} at the steel/solution interface[23-24].

To quantitatively evaluate the corrosion inhibition efficiency of the coating, ZSimpWin software was used to simulate and analyse the EIS spectrograms. And obtained equivalent circuit parameters are illustrated in Table 1.

Table 1. Equivalent circuit parameters of different coatings

Sample	$R_s/(\Omega \cdot \text{cm}^2)$	$R_1/(\Omega \cdot \text{cm}^2)$	$R_{ct}/(\Omega \cdot \text{cm}^2)$
Bare steel	3.344	18.76	142.7
Phytic acid	4.902	26.42	273.6
Post-treatment	5.151	412.9	1124.5

Generally speaking, the coating layer with high charge transfer resistance and low capacitance has good corrosion resistance to the metal substrate[25]. It is apparently concluded that the R_{ct} values of the coatings (bare steel, phytic acid coating and post-treated with a cerium nitrate solution of maximum concentration) were 142.7, 273.6 and 1124.5 $\Omega \cdot \text{cm}^2$, respectively, indicating that sample was post-treatment with cerium nitrate has better corrosion resistance against corrosive ion. Meanwhile, can be seen from the diagram, the radius of impedance spectroscopy enlarges with the increase of cerium nitrate concentration. This demonstrate that post-treated with cerium increased the corrosion reaction charge transfer resistance and retarded the sample corrosion rate. As evident from Table 1, the coating resistance and charge transfer resistance increases as post-treatment with cerium nitrate. The impedance of steel sheet which only coated with phytic acid increases slightly and the efficiency of that is 47.8 %, which is closed to that on other metal surfaces [16, 26]. When the concentration of cerium nitrate increased to 20 g/L, the efficiency is 87.3%. Fig.5 show respectively the bode modulus and bode phase representations of impedance data for the bare steel, phytic acid coated sample and post-treated with maximum concentration cerium nitrate conversion bath. The results show that cerium treatment increases the corrosion reaction charge transfer resistance and can effectively slow down the corrosion rate of the phytic acid coated sample

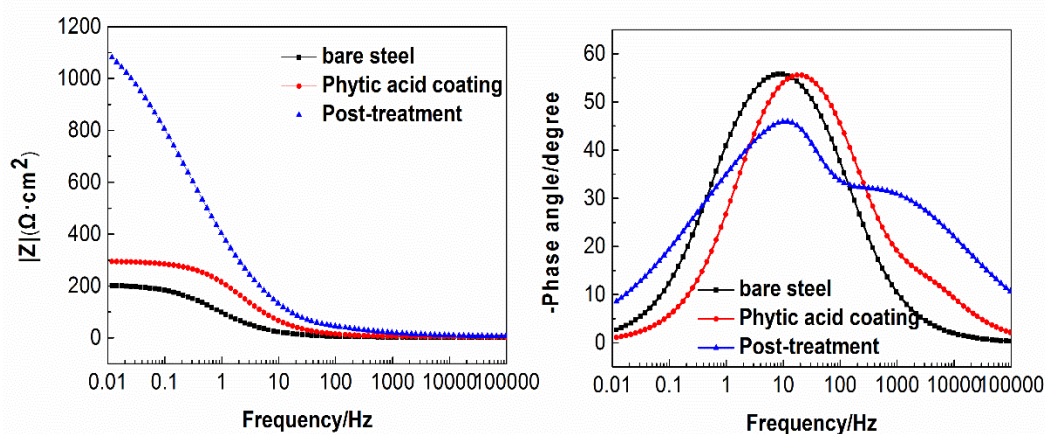


Figure 5. Bode and angle diagrams of phytic acid coating and phytic acid cerium salt composite coating

As can be seen from Table 1, the charge transfer resistance increases significantly with the increase of the concentration of cerium nitrate conversion solution. The resistance of cerium nitrate post-treatment coating increased nearly 5 times more than that of a single phytic acid coating. Bode plots provided information on the capacitive and resistant behavior of coated sample at different frequencies[27-28]. When phytic acid coated sample post-treated with cerium nitrate, the great changes of the impedance behavior were also observed from the corresponding Bode plots. Bode impedance spectra show that the corrosion process of steel involved only one time constant, which is related to the charge transfer process[29]. Whereas, when the steel treated with cerium nitrate, corrosion process involved two time constant for coated sample, which probably was associated with the relaxation process of the film resistance and the double layer capacitance at the micro-crack sites. These findings showed that post-treatment changed the anticorrosion mechanism. The results indicate

that there are two different transmission speed of the corrosive ions in the composite coating and the coating is mainly composed of phytic acid coating and cerium salt layer[15].

3.1.2 Polarization measurements of different conversion coatings

The polarization testing was also carried out on the coated samples to investigate the corrosion protection mechanism. Fig.6 presents the polarization plots of bare steel, PA coating and cerium nitrate post-treated coating. The corrosion current density (I_{corr}), corrosion potential (E_{corr}) and inhibition efficiency(E.%) were deduced from the polarization curves through the Tafel extrapolation technique and reported in Table 2.

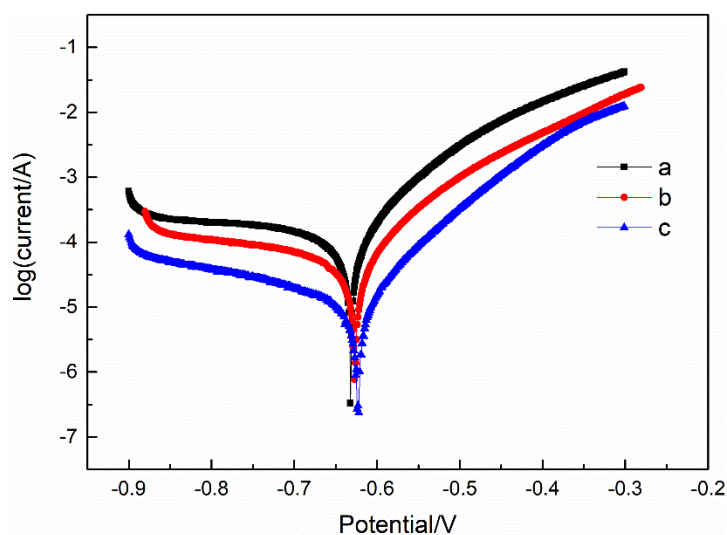


Figure 6. Polarization curves of different samples. a: bare steel; b: PA coating; c: composite coating

Table 2. Polarization parameters for the samples exposed to 3.5 wt% NaCl solution

Sample	I_{corr} ($\mu\text{A}/\text{cm}^2$)	E_{corr} (V)	E. (%)
Bare steel	142.6	-0.63	—
PA coating	49.57	-0.624	65.2
Composite coating	19.50	-0.619	86.3

A lower I_{corr} represents a sample with a better corrosion protection[30]. From Table 2, it is clearly seen that steel substrate surface treated by phytic acid coating and cerium nitrate post-treated coating resulted in a lower corrosion current density (I_{corr}) compared to the bare steel. Furthermore, the corrosion current density of the phytic acid coated steel was approximately three times larger than that post-treated sample, and that is a third of the corrosion current density of bare steel. This matter

indicates that the conversion coatings significantly retarded the corrosion rate of the steel samples. The deposition of phytic acid resulted in the corrosion potential (E_{corr}) being shifted towards a more positive value (from -0.632 V to -0.622 V) compared to the bare steel, showing that the phytic acid coating affected the anodic reaction more intensely than cathodic reaction. This finding shows that phytic acid reduced the corrosion rate of the bare steel through blocking the accessible active sites, especially the anodic sites on the steel surface. Whereas, the deposition of cerium salts resulted in the corrosion potential (E_{corr}) being shifted towards a more negative value compared to the bare steel, indicating that the composites coating affected the cathodic reaction more intensely than anodic reaction and shifted to a lower current density. Simultaneously, the cathodic reaction was obviously retarded via arresting the reduction of water, which was transported mainly through the micro-cracks of the coating. The protection efficiency of composites coating is consistent with that calculated with impedance method.

3.2 Characterizations of conversion coating

3.2.1 SEM and EDS

The surface morphologies of conversion coating were studied by SEM and the elemental composition of coated sample was characterized by EDS. The chemical composition of the specimen are depicted in Fig.7.

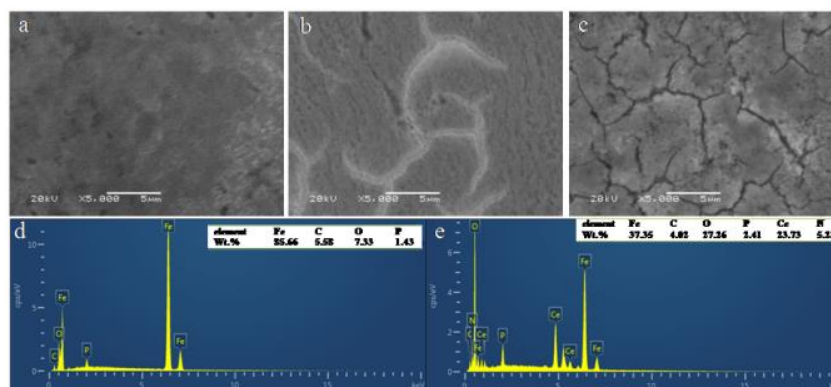


Figure 7. SEM images of samples. a) steel, b) phytic acid coating, c) cerium nitrate post-treatment and EDS images of samples. d) phytic acid coating, e) cerium nitrate post-treatment coating

Based on the Fig.7 d, it can be seen that the phytic acid conversion coating was mainly composed of Fe, C, O and P elements and the presence of P on the phytic acid coating shows that phytic acid chelate with the dissolution of metal ions and form a chemical conversion coating which can retard the diffusion rate of corrosive ions, such as the oxygen, Cl^- and H^+ ^[7-9]. The presence of element Ce on the coating demonstrated that phytic acid coating can continue to be treated by cerium nitrate. As seen in the Fig.7 a, the surface morphology of the bare steel is smooth, but a small amount of pits are observed because of occurred a slight corrosion during the placement. Nonetheless, there are some micro-cracks in the phytic acid coating sample. As seen in the Fig.7 c, the surface of the sample

that post-treatment with cerium nitrate was fully covered by the cerium conversion coating, but there were also has micro-cracks on the coating surface. Because in the process of preparation, phytic acid chelated with metal ions and led to the formation of hydrogen in the cathode part and those will cause a certain number of cracks appear. During the drying process, internal pressure of coating accelerates the results in the formation of micro-cracks that destroy the tightness of coating and seriously weaken the protective effect of coating to a certain degree.

3.2.2 XPS images

XPS measurement was performed to estimate the chemical state of elements present in the developed composite coating. The chemical station of P and Ce in the developed coating have analysed by XPS. The high-resolution XPS spectra of C 1s, P 2p, O 1s and Fe 2p_{3/2} on the phytic acid coated sample are listed in Fig. 8.

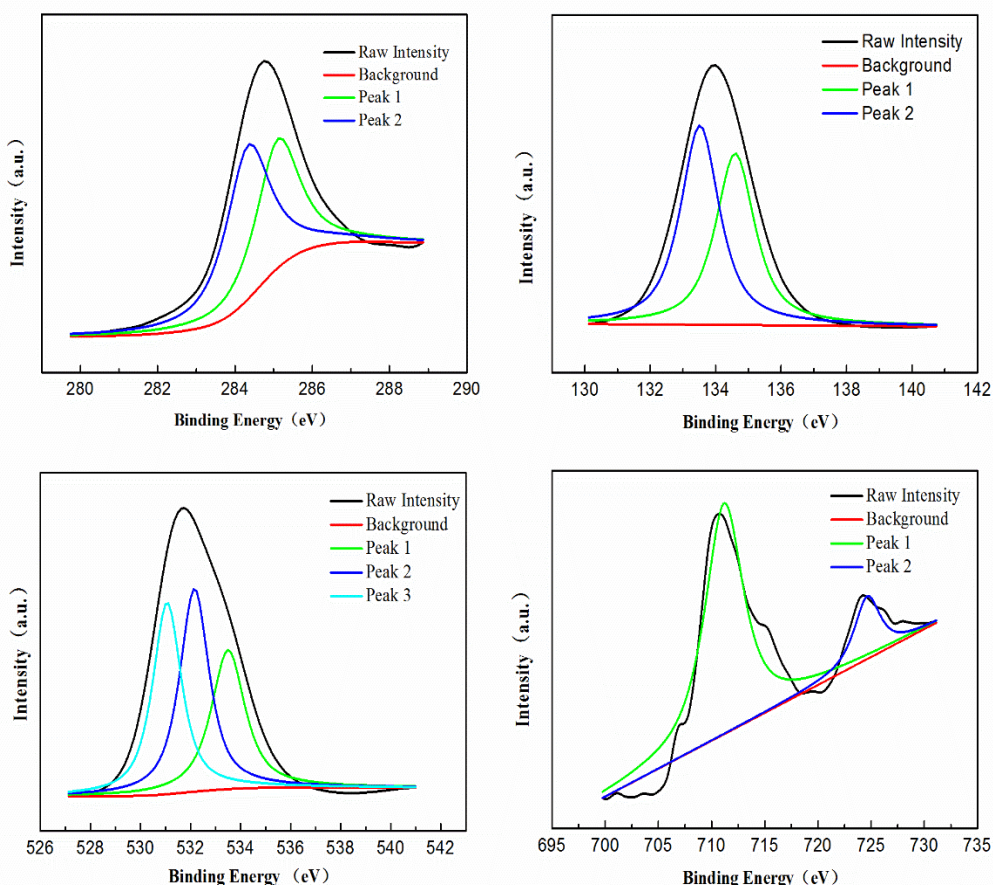


Figure 8. C(a), O(b), P (c) and Fe (d) XPS spectra of the formed phytic acid conversion coating under the optimized condition

The existence of carbon is common in XPS surface scan due to adventitious hydrocarbons from the environment. The full survey spectra of phytic acid coating(not shown) has revealed the presence

of O and P elements, which was consistent with the EDS result. The de-convolution of P 2p spectrum clearly shows that two peaks at binding energies of 133.5 eV and 134.6 eV corresponding to the chemical states: P-O-C and P-O-Fe[31]. This finding indicate that phytic acid chelate with iron to form a coating through the formation of P-O-Fe bonds. And these confirm the existence of phytic acid on steel surface. Form the O1s spectra, peaks around 530.1 eV, 532.2 eV and 533.4 eV are due to metal oxide peak, P=O and adsorbed water respectively. The Fe 2p_{3/2} region of phytic acid coating contains two peaks: a big peak located at around 711.2 eV appeared which corresponds to a type of ferric phytic acid complex[32]. This result confirms the formation of P-O-Fe bonds during the phytic acid deposition. The small peak located at 725.1 eV attributes to iron oxide (FeOOH) that the surface was not covered by phytic acid[33]. This pinpoints that the chelating reaction occurred between phytic acid molecules and Fe ions. About results obviously indicate that the phytic acid could bind to the steel surface through the formation of -P-O-Fe(III).

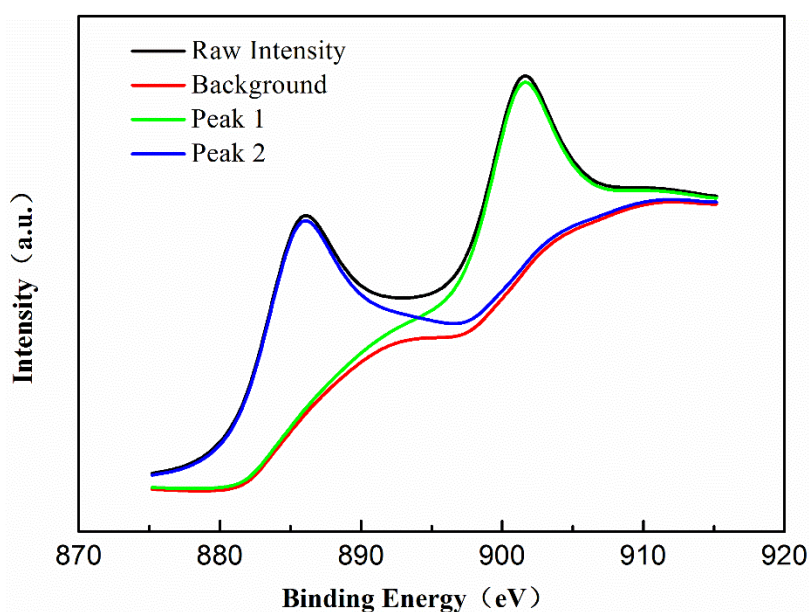
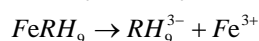
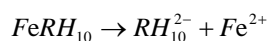


Figure 9. High resolution XPS spectra of Ce 3d for cerium post-treatment conversion coating

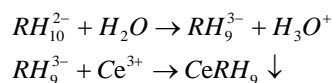
In the present study the developed composite coating contains Ce and hence, the Ce 3d was appeared at two different regions. Binding energies around 880–895 eV related to the Ce 3d₅ and around 895–910 eV associated with Ce 3d₃[34]. About results obviously indicate that the Ce was presented on the steel surface in the forms of both Ce³⁺ and Ce⁴⁺[35-36].

The obtained XPS spectra of composite coating confirms the formation of a composite coating on the steel surface. Hence, the plausible conversion coating formation mechanism of composite coating on Q235 steel surface is explained as follows:

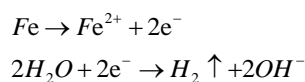
When the phytic acid coated sample is immersed in the cerium nitrate solution, the phytic acid that in the cracks will dissolve and occur the following reactions:



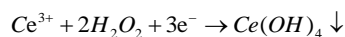
Then the RH_{10}^{2-} will ionize in the cerium nitrate conversion solution. And react with Ce^{3+} in the cerium nitrate conversion solution to form chelate compounds and deposit on the phytic acid coated sample surface [37].



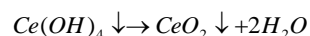
At the same time, the substrate which in the micro-cracks will dissolve and the cathodic reaction increases the OH^- ion concentration and results in localized pH rise.



In the meantime, increased in pH favors the oxidization of Ce^{3+} and precipitation of $Ce(OH)_4$ at the cathodic sites[38].



The existence of Ce^{4+} in the coating composition corresponds to the formation of CeO_2 . The decomposition reaction will occur when the composite conversion coating is exposed to air [39].



4.CONCLUSIONS

Cerium nitrate bath was used to treat phytic acid coated steel and the post-treatment steel had better corrosion resistance and better protection efficiency. The protection efficiency of the conversion coating increased with the increase of cerium nitrate concentration. The protection efficiency reached 87.3% when the concentration of cerium nitrate increased to 20 g/L. There were also has micro-cracks on the coating surface when post-treatment with cerium nitrate. XPS results indicated that the phytic acid could bind to the steel surface through the formation of -P-O-Fe and the Ce was presented on the steel surface in the forms of both Ce^{3+} and Ce^{4+} . In our view, more and more attention will be paid to not only improve the protective efficiency of the conversion film, but also endow it with certain self-repairing performance.

The phytic salts and cerium salts deposited together play a good shielding role, preventing the transmission of corrosive ions Cl^- , O_2 and H_2O to the metal surface. The denser the conversion coating formed, the higher the anti-corrosion efficiency.

CONFLICT OF INTEREST

The author confirms that this article content has no conflict of interest.

ACKNOWLEDGEMENTS

This research was financially support by China's ministry of science and technology" project for science and technology personnel service enterprise" (No.2009GJG10041).

References

1. N.W. Khun and G.S. Frankel, *Corrosion*, 71 (2015) 277.
2. B. Ramezanzadeh, M. Akbarian, M. Ramezanzadeh, M. Mahdavian, E. Alibakhshi and P. Kardar, *J. Electrochem. Soc.*, 6 (2017) 7.
3. J.A. Maga, *J. Agric. Food. Chem.*, 30 (1982) 9.
4. H. Wang, Y.M. Zhou, J.M. Ma, Y.Y. Zhou and H. Jiang, *Food Chem.*, 141 (2013) 18.
5. M. Zheng, Y.J. Cao, W.H. Cai, X. Shi, M.F. Wang and Y.J. Deng, *New J. Chem.*, 43 (2019) 11171.
6. B.L. Odell and J.E. Savage, *Proc. Soc. Experi. Biol. Med.*, 103 (1960) 3.
7. A. R. El-Sayed, U. Harm, K. M. Mangold and W. Fürbeth, *Corros. Sci.*, 55 (2012) 339.
8. L. Li, G. Zhang and Z. Su, *Angew. Chem.*, 55 (2016) 5.
9. H. Ejima, J.J. Richardson, K. Liang, J.P. Best, M.P. Koeverden, G.K. Such, J. Cui and F. Caruso, *Science*, 341 (2013) 154.
10. H.W. Shi, E. H. Han, F.F. Liu and S. Kallip, *Appl. Surf. Sci.*, 280 (2013) 325.
11. X.F. Cui, Q.F. Li, Y. Li, F.H. Wang, G. Jin and M.H. Ding, *Appl. Surf. Sci.*, 255 (2008) 2098.
12. M. Becker, *Corros. Rev.*, 37 (2019) 32.
13. R.Y. Zhang, S. Chen, G.H. Xu, H. Zhang, Y.Li, X.X. Wang, K. Hu, M.G. Rui and X.D. Wu, *Appl. Surf. Sci.*, 313 (2014) 896.
14. H.F. Gao, H.Q. Tan, J. Li, Y.Q. Wang and J.Q. Xun, *Surf. Coat. Techn.*, 212 (2012) 32.
15. J.R. Liu, Y.N. Guo and W.D. Huang, *Prot. Met. Phys. Chem.*, 48 (2012) 233.
16. H.E. Mohammadloo and A.A. Sarabi, *Prog. Org. Coat.*, 101 (2016) 391.
17. L.H. Yang, J.P. Li, X. Yu, M.L. Zhang and X.M. Huang, *Appl. Surf. Sci.*, 255 (2008) 2338.
18. S.S. Jamali, S.E. Moulton, D.E. Tallman, Y. Zhao, J. Weber and G.G. Wallace, *Electrochem. Commun.*, 76 (2017) 6.
19. D.Z. Zhao, D.F. Zhang, Y.P. Liu, G.S. Hu, Y.N. Gou and F.H. Pan, *Rare Metal Mat. Eng.*, 46 (2017) 7.
20. E.J. Ruiz, R. Ortega-Borges, L.A. Godínez, T.W. Chapman and Y. Meas-Vong, *Electrochem. Acta*, 52 (2006) 914.
21. B.J. Han, *Int. J. Electrochem. Sc.*, 12 (2017) 374.
22. D. Dwivedi, K. Lepková and T. Becker, *RSC Adv.*, 7 (2017) 4580.
23. M. Gobarra, A. Baraka, R. Akid and M. Zorainy, *RSC Adv.*, 10 (2020) 2227.
24. N. Dang, Y.H. Wei, L.F. Hou, Y.G. Li and C.L. Guo, *Mater. Corros.*, 66 (2015) 1354.
25. M. Garcia-Heras, A. Jimenez-Morales, B. Casal, J.C. Galvan, S. Radzki and M.A. Villegas, *J. Alloy. Comp.*, 15 (2004) 380.
26. R. Yan, X. Gao, W. He, R. Guo, R.N. Wu, Z. Z. Zhao and H. Y. Ma, *RSC Adv.*, 7 (2017) 41152.
27. J. Kittel, N. Celati, M. Keddani and H. Takenouti, *Prog. Org. Coat.*, 46 (2003) 135.
28. B.R. Hinderliter, S.G. Croll, D.E. Tallman, Q. Su and G.P. Bierwagen, *Electrochim. Acta*, 51 (2006) 4505.
29. X. Jiang, R. Guo and S. Jiang, *J. Magnes. Alloy.*, 4 (2016) 230.
30. A. Adhilakshmi, K. Ravichandran and T.S.N. Sankara Narayanan, *New J. Chem.*, 42 (2018) 18458.
31. E. Smecca, A. Motta, M.E. Fragalà, Y. Aleeva, G.G. Condorelli, *J. Phys. Chem. C.*, 117 (2013) 5364.
32. R. Cai, H. Liu, W.Y. Zhang, H.T. Tan, D. Yang, Y.Z. Huang, H.H. Han, T.M. Lim and Q.Y. Yan, *Small*, 9, (2013) 1036.
33. X. Gao, K. Lu, L. Xu, H. Xu, H.F. Lu, F. Gao, S.F. Hou and H.Y. Ma, *Nanoscale*, 8 (2016) 1555.

34. B. Ramezanzadeh, H. Vakili and R. Amini, *J. Ind.Eng. Chem.*, 30 (2015) 225.
35. J.M. Sánchez-Amaya, G. Blanco, F.J. Garcia-Garcia, M. Bethencourt and F.J. Botana, *Surf. Coat. Tech.*, 213 (2012) 105.
36. A. Uhart, J.B. Ledeuil, D. Gonbeau, J.C. Dupin, J.P. Bonino, F. Ansart and J. Esteban, *Appl. Sur. Sci.*, 390 (2016) 751.
37. A. J. Aldykiewicz, A.J. Davenport and H.S. Isaacs, *J. Electrochem. Soc.*, 143 (1996) 8.
38. X.W. Yu and G.P. Li, *J. Alloys Compd.*, 364 (2004) 193.
39. S. Joshi, E.A. Kulp, W.G. Fahrenholtz and M.J. O'Keefe, *Corros. Sci.*,60 (2012) 290.

© 2020 The Authors. Published by ESG (www.electrochemsci.org). This article is an open access article distributed under the terms and conditions of the Creative Commons Attribution license (<http://creativecommons.org/licenses/by/4.0/>).